

MDU: A Model for Dynamic Upscaling

Roland Lenormand and Darryl Fenwick
Institut Français du Pétrole, Rueil-Malmaison France

"All models are wrong, but some are useful"

Abstract

The purpose of this study is to replace numerical two-phase upscaling by an analytical calculation of the average properties. Our approach is based on homogenization of the saturation (or fractional flow) profiles instead of permeability. The complicated saturation field is replaced by a smooth one, described by a homogenized transport equation. The smoothing procedure follows two constraints: same spreading of the front and same behavior of extreme cases of random and perfectly layered fields.

We first introduce results from several tracer displacements in heterogeneous media. We propose an alternate approach based on the fractional flow instead of Darcy's law. Instead of relative permeability and capillary pressure, our approach introduces a homogenized form of the fractional flow and a homogenized pressure equation.

When deriving the general transport equation, we define two new functions, $F_c(S)$ and $F_d(S)$, where S is the saturation of a given fluid. F_c and F_d are defined as the convective and dispersive fractional flows respectively. When the porous medium is homogeneous, F_c and F_d reduce to the standard expressions in Darcy's equations. In the case of tracer displacement in a heterogeneous permeability field, we show that F_c and F_d can be predicted as function of the stochastic properties of the permeability field. For miscible displacements, we indicate how our new approach can be connected to previous work concerning viscous fingering. Finally, we indicate how our new approach can be directly used in existing reservoir simulators, by calculating pseudo relative permeabilities and capillary pressures using the functions F_c and F_d .

1. Introduction

Powerful geostatistical algorithms conditioned to log and core measurements make it possible to generate geological images with a pixel resolution for permeability and porosity on the orders of centimeters. Interwell distances and field dimensions, on the other hand, are on the order of hundreds of meters and kilometers respectively. Field-scale numerical modeling of fluid flow using fine-scale information would therefore result on the order of 10^{12} grid blocks, which is well beyond current computational resources. As a result, simulations have to be performed on larger grid blocks with average properties derived from the underlying fine-grid information. This operation, called "upscaling" is still a limitation in reservoir simulations. The

purpose of this paper is to present the framework and preliminary results for a new approach for dynamic two-phase upscaling.

The main idea governing our approach is that upscaling must be considered as the result of two different operations: homogenization and discretization. Upscaling in the petroleum industry is always presented in a discrete approach, starting from a fine grid description of the permeability field (typically 10 meters) to a coarse grid (100 m). Even if this approach represents the real problem, there is no theoretical tool to calculate flow properties at two different grid sizes. We need to use, as intermediate, the continuum approach where the transport equations are known. Consequently, we propose the following two-stage approach represented in Fig. 1:

- 1) At the small scale, the transport properties are governed by the standard two-phase Darcy’s equations for pressure and the mass balance equation (see Marle). Assuming Darcy’s law means that relative permeabilities K_r and capillary pressure P_c depend on saturation only (for a given displacement, drainage or imbibition). The medium is heterogeneous with a permeability field described by a continuum function $K(x,y,z)$. We are considering a dynamic process, i.e. a fluid is displacing another one (waterflood for instance). The invasion front of the injected fluid will spread due to the change in local properties (K , K_r , P_c , etc.).

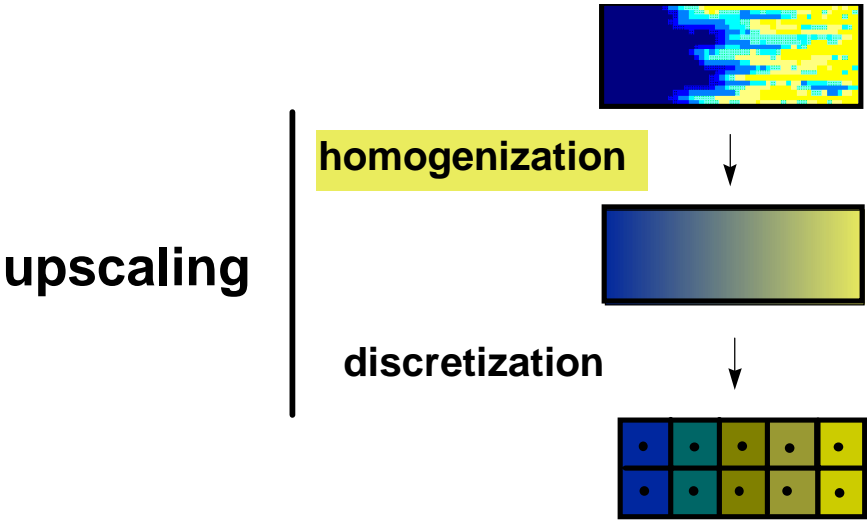


Fig. 1- Principle of MDU approach for upscaling

- 1) The saturation field is homogenized. The main difference with the discrete approach is that we do not homogenize the permeability field but the saturation field directly. The complicated saturation field is replaced by a smooth one, described by a homogenized transport equation. The smoothing procedure, follows some constraints that depend on the problem and will be described later. Note that the homogenized saturation and transport equation are still described in the continuum context.
- 2) For numerical simulations, the medium is discretized. This discretization introduces an error due to the non-uniformity of the saturation inside a grid block (at the difference with continuum approach). The error, called numerical dispersion, increases with grid block size and also the gradient of saturation. Note that this kind of numerical

dispersion should be differentiated from the numerical dispersion caused by truncation error of the governing equations. Numerical dispersion can be corrected by changing the properties of the homogenized transport equation.

To summarize our approach, there are two steps: front homogenization and discretization. In this paper, we focus on homogenization.

We first introduce results from several tracer displacements in heterogeneous media. We analyze the results, and show why Darcy's law cannot be used for an homogenized transport equation. We propose an alternate approach based on the fractional flow instead of Darcy's law. Instead of relative permeability and capillary pressure, our approach introduces a homogenized form of the fractional flow and a homogenized pressure equation. The homogenized fractional flow equation can be of two forms:

- 1) as a function of distance and time, $f(x,t)$
- 2) as a function of saturation $f(S)$, which combined with the mass balance equation leads to a general transport equation

When deriving the general transport equation, we define two new functions, $F_c(S)$ and $F_d(S)$, where S is the saturation of a given fluid. F_c and F_d are defined as the convective and dispersive fractional flows respectively. When the porous medium is homogeneous, F_c and F_d reduce to the standard expressions in Darcy's equations. In the case of tracer displacement in a heterogeneous permeability field, we show that F_c and F_d can be predicted as function of the stochastic properties of the permeability field. For miscible displacements, we indicate how our new approach can be connected to previous work concerning viscous fingering. Finally, we indicate how our new approach can be directly used in existing reservoir simulators, by calculating pseudo relative permeabilities and capillary pressures using the functions F_c and F_d .

2. Model for Dynamic Homogenization

In this section, we will present our new model, based on the results of various fluid displacements in heterogeneous media. Since real experiments are not easy to perform in heterogeneous media, we will use numerical simulations. However, the numerical experiments are assumed to represent the continuum, and are not presented as giving a result at a specific (small) grid size.

2.1 Numerical experiments

The local simulations are similar to those described by Lenormand and Thiele (1996). We perform cross-sectional displacements with an injector at one end and a producer on another. The injector is at constant flow rate, and the producer is at constant pressure. The fluids in the displacement are incompressible.

2.1.1 local properties

The 2-dimensional permeability fields were created by using GSLIB (Deutch and Journel, 1992) and contain 250x100 gridblocks. We used exponential variograms and a lognormal permeability distribution. We considered four different correlation lengths (normalized by the length of the medium): $\lambda=0.01, 0.1, 1, \text{ and } 10$, and permeability variance $\sigma^2(\log K)=1$. Example permeability fields are shown in Fig. 2.

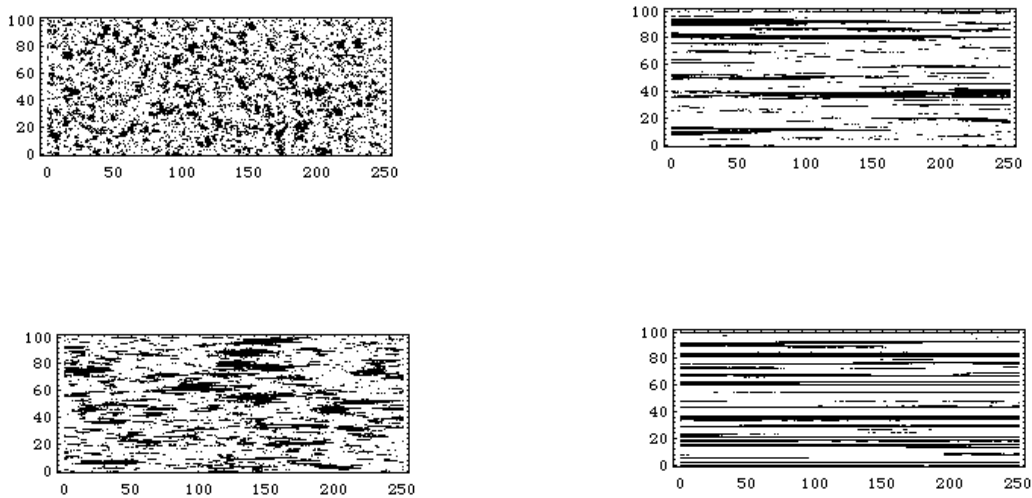


Fig. 2 - Examples of permeability fields used for the simulations

At the local scale, the flow of fluids 1 and 2 are governed by Darcy's law

$$u_1 = \frac{K K r_1}{\mu_1} (-\nabla P_1)$$

$$u_2 = \frac{K K r_2}{\mu_2} (-\nabla P_2)$$

$$P_c(S) = P_2 - P_1$$

where u is the flow rate per unit cross-sectional area, ∇P is the gradient of the pressure, and μ is the viscosity (all other terms as previously defined).

In the simulations presented in this paper, there is no local capillary pressure. The relative permeabilities are simple power laws with different exponents (Corey functions with exponents 1, 2, or 3, see Fig. 3). Saturation used in our simulations can be seen as a rescaled saturation, with zero initial and final saturations. The case of relative permeability with the Corey exponents equal to unity can be considered as a tracer case without any molecular diffusion or microscopic dispersion. At local scale, the displacement is piston-like and the large scale spreading is only caused by the heterogeneity. The tracer case will be studied in detail as it is often a simple and efficient way to sample and measure the heterogeneity of the field. The viscosity ratio (M =viscosity of displaced fluid/viscosity of injected fluid) is either 1 or 5. Displacing fluid is injected continuously at time $t=0$. It is important to note that the transport equations derived in this paper are valid only for this type of displacement.

2.1.2 numerical simulations

The simulations were performed using 3DSL, a streamline simulator developed at Stanford University (see Batycky, Blunt, and Thiele, 1997). 3DSL has been shown to produce results up to 1000 times faster than standard industry simulators with a minimum of numerical dispersion (error due to discretization). Simulation speed and precision were of the utmost importance for

the simulations presented below. It was necessary at times to inject over 100 pore volumes in some cases, which would have taken many weeks with standard reservoir simulators instead of less than a day with 3DSL. Additionally, we found that the numerical dispersion using standard simulators severely impacted upon the results, and the use of 3DSL became essential. Some simulations are also performed using ATHOS, the IFP reservoir simulator.

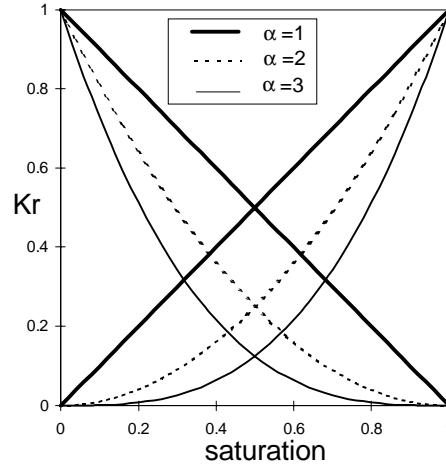


Fig. 3 - Relative permeability curves used for the numerical simulations

2.1.3 homogenization rules

The geometry of a cross-sectional displacement is a quasi linear problem when gravity is neglected. Consequently, we seek to homogenize saturation as function of x only, smoothing all the fluctuations in the y -direction. From the numerical experiments, we integrate the saturation over the y -direction and derive the experimental average saturation, as is shown in Fig. 4. It is evident in Fig. 4 that the homogenized saturation obtained as a solution of a transport equation cannot reproduce all the fine details of the average saturation. However, the homogenized saturation can be constrained to reproduce certain characteristics of the average saturation. In our approach, we constrain the homogenized saturation to the first and second moments (i.e. mean and variance) of the fine detail average saturation profile. Thus, the homogenized saturation profile must then have the same mean and variance as the experimental profile.

The first moment is the mean velocity of the front and is defined by (Lenormand and Thiele, 1996)

$$\langle x \rangle = \int_0^L x \frac{\partial S}{\partial x} dx$$

The variance characterizes the spreading of the saturation

$$\sigma_s^2(t) = \int_0^L (x - \langle x \rangle)^2 \frac{\partial S}{\partial x} dx$$

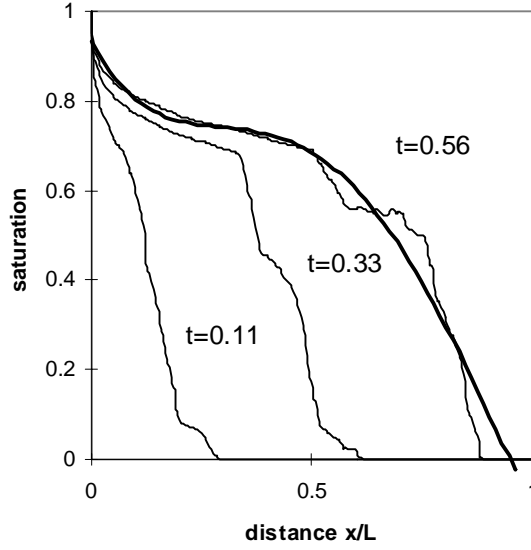


Fig. 4 - Saturation profile at three different times for water displacing oil, Corey exponents of 3, $\lambda=0.1$, $\sigma^2(\log K)=1$. The curve in bold is an homogenized saturation profile.

In fact, we will generally use the fractional flow f instead of saturation ($f=u_1/u_1+u_2$). But the principle is the same since there is a duality between the two variables through the mass balance equation. For 1-dimensional incompressible flow

$$\frac{\partial S}{\partial t} + u \frac{\partial f}{\partial x} = 0$$

Thus, instead of spatial moments with saturation, we use temporal moments with the fractional flow

$$\langle t \rangle = \int_0^\infty t \frac{\partial f}{\partial t} dt$$

The variance characterizes the spreading of the fractional flow

$$\sigma_f^2(x) = \int_0^\infty (t - \langle t \rangle)^2 \frac{\partial f}{\partial t} dt$$

Compared to saturation, using fractional flow presents two main advantages

- 1) Numerical simulations are not limited at breakthrough. For spatial moments part of the injected fluid is lost after breakthrough and the moments are not longer exact. For temporal moments, simulations can be continued after breakthrough until all the fluid is displaced from the sample, as in a real experiment (sometimes after flowing more than 100 pore volumes).
- 2) Fractional flow is directly related to the notion of arrival time used in stochastic calculations. This property will be useful when considering tracer displacements.

To summarize, we will use the following rules for homogenization, based on fractional flow

- 1) the 1st moment (mean) is the same in the local and homogenized description

2) the variance, i.e. spreading of the front is the same at any distance.

2.1.4 some results and interpretation - tracer

In this section we show the results of the variance (of fractional flow) at different positions x . For the simplest case of displacement of a non-diffusive tracer (i.e. Corey exponent of 1) in a heterogeneous media, a tremendous amount of previous work has been published. Essentially, the variance for this displacement has one of three types of behavior:

- 1) $\sigma_f^2 \sim x$, which corresponds to dispersive spreading due to short range correlations in the heterogeneity field (macrodispersion). We denote this the dispersive regime.
- 2) $\sigma_f^2 \sim x^2$, which corresponds to convective spreading linked to channeling (i.e. long range correlations). This is the convective regime.
- 3) $\sigma_f^2 \sim x^\beta$, where $1 < \beta < 2$, which corresponds to an intermediate regime between convection and dispersion (anomalous dispersion, see Glimm et al., 1993).

We have performed several tracer simulations on the four permeability fields shown in Fig. 2, as well as a perfectly layered field ($\lambda = \infty$) and an uncorrelated field ($\lambda = 0.004$). The variances of the flux scaled by the maximum variance of the simulation (at the producing well) are shown in Fig. 5. For the layered case, the calculated variances fall on a line of slope 2 on the log-log plot (and thus $\sigma_f^2 \sim x^2$). For the cases of low correlation length, we also note that the points fall close to a slope of 1. For the intermediate cases, we can see that the simulation results can be accurately fitted with a straight line of slope β , where $1 < \beta < 2$. The relationship $\sigma_f^2 \sim x^\beta$ for non-dispersive tracer flow has been proposed by several authors to describe dispersion in strongly heterogeneous media. This approach leads to integrodifferential equations or fractional derivatives that are not easy to use in the framework of reservoir simulators (Lenormand, 1992).

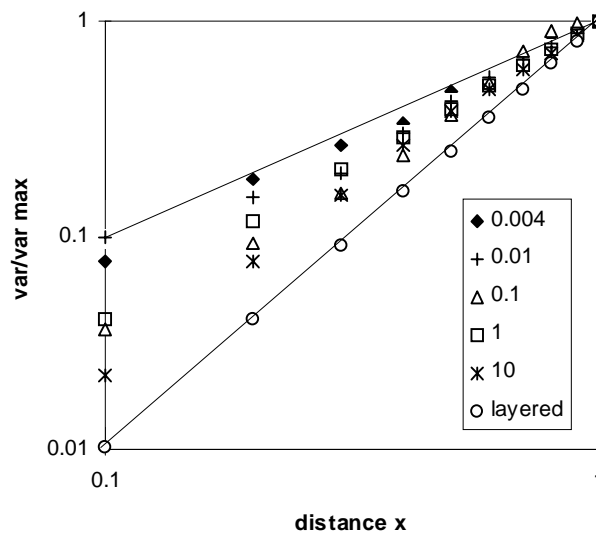


Fig. 5 - Flux variance as function of distance for various types of displacements

Instead of expressing the variance as $\sigma_f^2 \sim x^\beta$, Lenormand and Thiele (1996) proposed that the variance can be expressed by a quadratic function,

$$\sigma_f^2(x) = A x^2 + B x$$

Clearly, for the two extreme cases the quadratic expression is exact. We have found as well that a quadratic expression fits well to all intermediate cases investigated. As an example, Fig. 6 shows the experimental variance for the intermediate case of $\lambda=1$, and the best fits of $\sigma_f^2(x)$ using power law and quadratic expressions.

We have only shown results for tracer flow. However, the approach is valid for immiscible flow as well. Fig. 7 presents $\sigma_f^2(x)$ for water displacing oil with Corey exponents of 2 in a permeability field with $\lambda=0.1$, $\sigma^2(\log K)=1$. Again, the quadratic expression is quite appropriate in describing $\sigma_f^2(x)$.

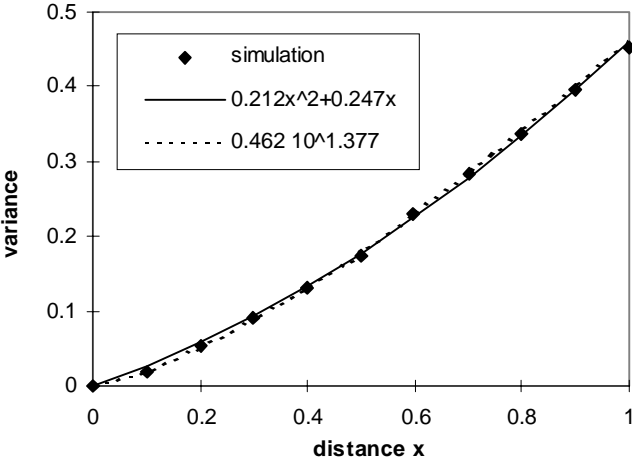


Fig. 6 - Approximation of variance by different laws for $\lambda=1$. The quadratic equation is $0.2121x^2+0.2475x$ and the power law $0.4616x^{1.3772}$.

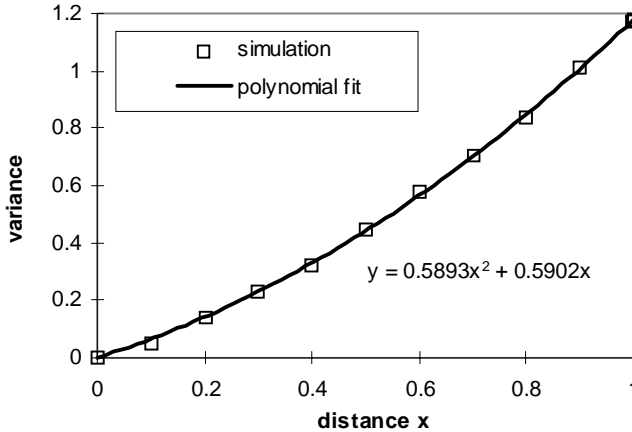


Fig. 7 - Displacement in a permeability field with $\lambda=0.1$, $\sigma^2(\log K)=1$ and local relative permeability (Corey exponent $\alpha=2$) and fit using a 2nd order polynomial

Using the quadratic expression for the variance has the advantage because we can separate out the convective and dispersive contributions to the flow, allowing us to empirically define a fractional flow, and thus homogenized transport equation.

2.2 General homogenized transport equation

The first approach in determining a homogenized transport equation is to use the same form as at the local scale. Quintard and Bertin (1989) used a volume averaging method to demonstrate the validity of Darcy's law in the quasi-static limit. The pressure is then uniform in the two fluids and the effective capillary pressure curves $\langle P_c \rangle$ can be derived from the local P_c curves. The average relative permeability are also derived.

For the large majority of cases where the displacement is not in quasi-static equilibrium, Darcy's law can no longer be used for the dynamic regime. Here we explain why.

2.2.1 limit of Darcy's law

The first problem stems with the definition of pressure. Even without capillary effects, the pressure differs from point to point due to local variations in permeability. It is also true for other variables such as saturation and flux. However, the main difference is that pressure is not an extensive variable and there is no physical means to define an average pressure. The average pressure has to be defined using relationships with saturation or fractional flow, which are extensive variables (in fact, the extensive variables are volume, mass and cross-section area, used to define S and f).

The second limit of Darcy's equations concerns the variance of the front. When we homogenize, we constrain the variance of the fractional flow such that it scales the same with distance as the averaged one. This is not possible in general using Darcy's approach. The scaling of variance with distance is not correct. For example, displacement in a field with $\lambda \ll L$ (L is the length of our displacement), even with no P_c , will be characterized by a spreading in Ax^2+Bx , with a strong contribution of the dispersive term B due to dispersive effects of the heterogeneity. If we homogenize using Darcy's law, we would be using the standard Buckley-Leverett equation which uses an "effective" relative permeability $\langle K_r \rangle$ to capture the effect of the heterogeneity. However, the Buckley-Leverett equation is purely convective, where $\sigma_f^2 \sim x^2$. Consequently, to match $\sigma_f^2(x)$ at all x with a single curve for $\langle K_r \rangle$ is impossible when we have dispersion (i.e. $B \neq 0$). This problem of validity of Darcy's law has also been discussed by Chang and Mohanty (1994).

In order to overcome this problem, one can introduce space dependent $\langle K_r \rangle$. This is difficult to implement in numerical simulators. Another possibility is to use a fictitious capillary pressure $\langle P_c \rangle$ to account for the dispersive contribution in the variance. Following a more general approach, we propose a model without using the terms of $\langle K_r \rangle$ and $\langle P_c \rangle$.

2.2.2 fractional flow function

We now propose the general form of fractional flow

$$f = F_C(S) - F_D(S) \frac{\partial S}{\partial x}$$

where F_C and F_D are functions of saturation only and characterize convective and dispersive spreading, respectively. The fractional flow is homogenized when $F_C(S)$ and $F_D(S)$ are defined such that the mean and variance of the local and homogenized description are the same.

Using the mass balance leads to the homogenized transport equation

$$\frac{\partial S}{\partial t} + u \frac{\partial F_C}{\partial x} = \frac{\partial}{\partial x} \left(F_D \frac{\partial S}{\partial x} \right)$$

In this equation, F_C and F_D are two homogenized functions that replace the local K_r and P_c . They must be determined either by fine grid numerical simulations or analytical calculation. We will give some examples of calculation of F_C and F_D in the rest of the paper.

In the standard discrete approach, Darcy's pressure equations are used with the definition of capillary pressure, and the fractional flow is then derived. In our approach, the form of fractional flow is assumed a priori. Thus, we need additional assumptions concerning the pressure.

2.2.3 pressure function

The determination of pressure can be done in one of several ways. We do not explore this issue in depth, but only mention several possibilities for future research. Essentially, the problem is that we need to determine the total velocity u for the fluids, which can then be substituted into the generalized transport equation.

One possibility is to keep two pressures as in the standard approach. This approach is necessary for the experimental determination of capillary properties of heterogeneous core samples.

The second possibility is to define an "effective" pressure. This pressure can be defined empirically as a function of saturation or fractional flow, depending on the problem. This has the advantage in that there is no need for the two fluids to be continuous (trapped phase, flow of ganglia, emulsions), and can also be extended to flows where inertia is important. This is similar to an approach used for flow in chemical reactors and for two-phase flow in pipes.

In the next section, we show how our Model for Dynamic Upscaling (MDU) is coherent with standard approach for homogeneous media. Then, we consider the simplest case of tracer displacement in heterogeneous media, without local mixing.

3. Application to homogeneous media

In this section, we will show that our new approach is not incompatible with standard approach when the medium is homogeneous.

3.1 Two-phase flow

In homogeneous medium with permeability K , the fractional flow is directly derived from Darcy's equations and convective and dispersive fractional flow are easily identified to

$$F_c = \frac{\mu_2 / Kr_2}{\mu_2 / Kr_2 + \mu_1 / Kr_1} \quad ; \quad F_d = \frac{AK}{Q} \frac{1}{\mu_2 / Kr_2 + \mu_1 / Kr_1} \frac{\partial Pc}{\partial S}$$

For the pressure equation, if we use only one pressure in this case (such as the pressure of the injection phase), we lose some accuracy of the pressure description. However, if we use both pressures the approach using F_c and F_d is exactly the same as using Darcy's law.

3.2 Miscible flow - viscous fingering

When the injected fluid is completely miscible in the invaded fluid, and the mixture of the two fluids has a lower viscosity than the invaded fluid, viscous fingering can occur. This is drawn schematically in Fig. 8. There are no analytic solutions to the fractional flow for viscous fingering. However, Koval (1963) proposed an expression for the fractional flow, which, when reduced to our generalized form is

$$F_c = \frac{S}{S + (1-S)/M^*} \quad ; \quad F_d = 0$$

where M^* is an effective viscosity ratio. Thus, viscous fingering is modeled as convective, with no dispersive component. This empirical equation has been shown to model the flux of first-contact miscible displacements accurately. Koval's fractional flow is shown in Fig. 9 as a function of saturation and time.

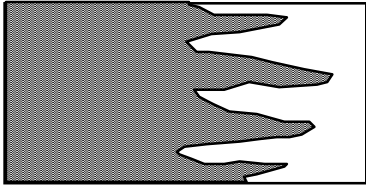


Fig. 8 - Schematic saturation map for viscous fingering in a homogeneous medium

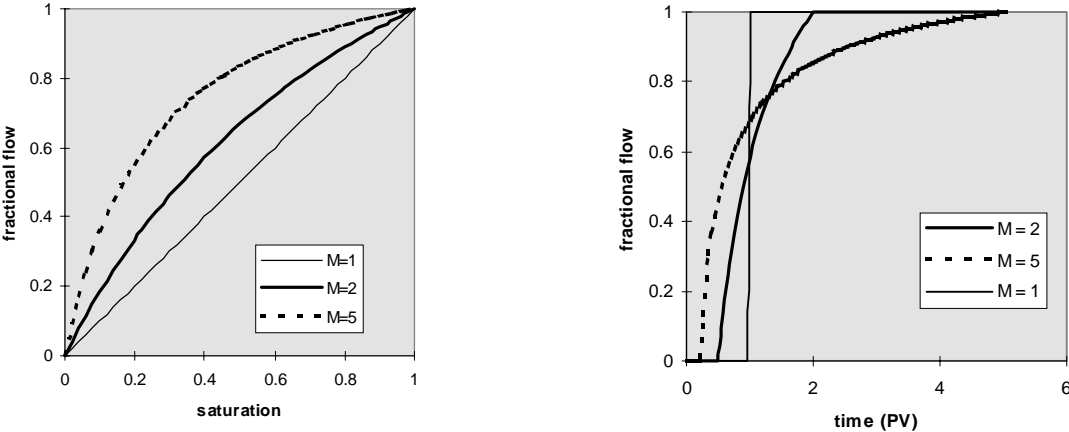


Fig. 9 - Fractional flow as function of saturation and time for the Koval's function representing viscous fingering in a homogeneous medium

For pressure equation, we can use an effective viscosity (or mobility) approach such as the one proposed by Todd and Longstaff (1972).

We will come back to the Koval expression again and take advantage of its properties when we examine tracer displacements in heterogeneous media.

4. Application to tracer displacements

In this section, we derive fractional flow functions based upon the two extreme cases of pure dispersion and pure convection. We use published results to obtain the variance of the front spreading which we use to constrain our flux expressions. Two different models are proposed:

- 1) the calculation of an homogenized form for the fractional flow $f(x,t)$, using a physical model based on streamtubes and separation of scales
- 2) an empirical formulation for the fractional in terms of $F_c(S)$ and $F_d(S)$ in the MDU framework, leading to a homogenized transport equation.

4.1 Variance of front spreading - theory

We will use the results published by Lenormand (1995) and Lenormand and Wang (1995) The principle is to solve a 1-dimensional displacement problem inside streamtubes instead of a more complicated 3-D problem (Gelhar and Axness 1983). All the streamtubes are filled at constant flow rate and spreading stems from the local variation in tube section (and therefore in volume). With some assumptions such as vertical equilibrium, a simple relationship can be derived between local permeability, volume of the streamtube and time for filling this volume. Spreading can be characterized by the arrival time of the front which is related to variance and correlation of filling times. The process can be described by "continuous time random walk" rather than standard random walk.

For exponential variogram, with correlation length λ , variance of arrival times, or fractional flow with our notations is

$$\sigma_f^2 = \frac{2\lambda^2}{u^2} \left(\frac{x}{\lambda} - 1 + e^{-x/\lambda} \right) \sigma_{\text{LogK}}^2$$

The two extreme cases are easily derived by taking the limits of the exponential. For random media with short correlation length, the result is similar to the result of Gelhar and Axness (1983)

$$\lambda \ll x \quad ; \quad \sigma_f^2 = \frac{2\lambda}{u^2} x \sigma_{\text{LogK}}^2$$

For stratified media

$$\lambda \gg x \quad ; \quad \sigma_f^2 = \frac{1}{u^2} x^2 \sigma_{\text{LogK}}^2$$

The general expression for exponential field agrees well with numerical simulations in Fig. 10. In Fig. 10 we scale the variance by the theoretical result of Gelhar and Axness (1983) and plot the scaled variance as a function of the ratio of the actual distance x divided by the correlation length λ . There is not complete agreement due to several factors. The most important are:

- 1) The actual correlation length and variogram shape of the simulated permeability field are not identical to the input variogram used to calculate the theoretical variance,
 - 2) The theory is for a continuous description of the permeability field, whereas the simulations were performed on a discrete field,
 - 3) The theory makes some approximations in order to obtain its analytic form.
- Nevertheless, the results are satisfactory.

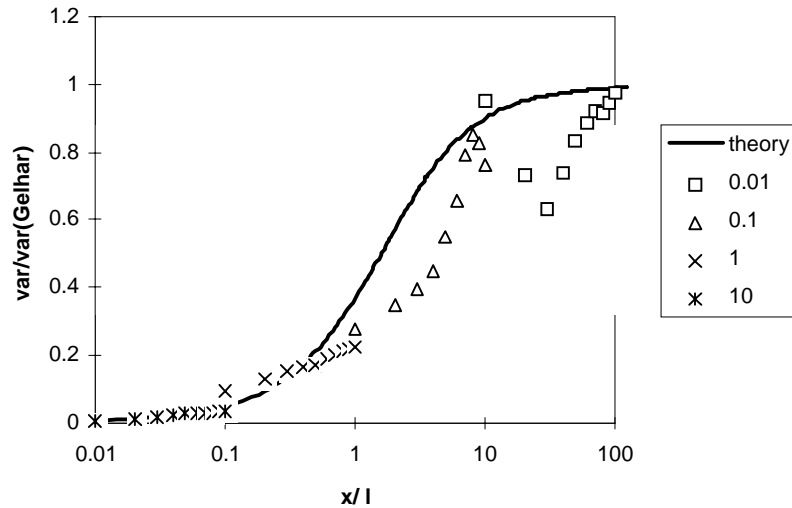


Fig. 10 - Variance for the fractional flow at various distances: comparison between theory and numerical simulations

The theoretical variance of fractional flow has also been established for other types of variograms (Lenormand and Wang, 1995). For instance, a power law variogram with exponent β leads to a variance that scales as $x^{(2-\beta)}$, a result also derived by Glimm.

4.2 Calculation of homogenized fractional flow

So far, we have used a stochastic approach to derive scaling laws for front spreading, i.e. the variance of fractional flow as function of traveled distance. However, we want to derive a transport equation or the fractional flow itself, and not only its variance. There is not enough information in the variance to derive the fractional flow function, and the whole set of moments is needed in general. In our approach, we do not use higher order moments, but constrain the fractional flow using the two limits of purely dispersive and purely convective displacements.

4.2.1 Extreme cases

To visually demonstrate our approach, we show in Fig. 11 the fractional flows at the producing well for a continuous injection of tracer into the given permeability fields.

For the limiting case of short correlation length ($\lambda=0.01$), the displacement is described by a standard dispersion equation (Gelhar and Axness, 1983). The fractional flow functions are $F_c=S$ and $F_d=D$ and the solution follows an error function.

$$f(x,t) = \frac{1}{2} \left(\operatorname{erf} \left(\frac{t - x/u}{2 \frac{x}{u} \sqrt{D/x}} \right) + 1 \right)$$

For the limiting case of layering ($\lambda=10$), the curve is similar to the function proposed for viscous fingering seen in Fig. 9. For both viscous fingering and tracer in layered field, the fractional flow as functions of saturation have the same shape, with f always greater than S . To demonstrate, Fig. 12 shows the fractional flow for a perfectly layered permeability field of uniform distribution of $1/K$ between two values $1/K_{\max}=0.4$ and $1/K_{\min}=1.6$. Fig. 12 also includes an approximation by a function of the form

$$F_c = \frac{S}{S + (1-S)/H}$$

which heterogeneity index H fitted to $H=1.95$ (Lenormand, 1996).

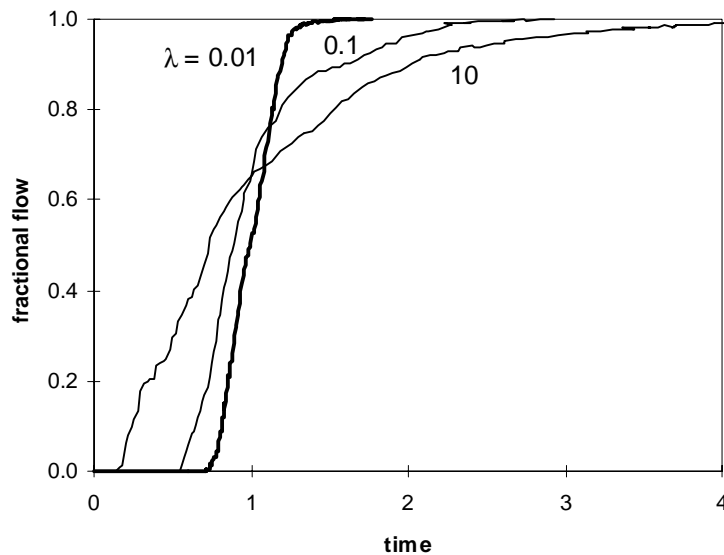


Fig. 11 Fractional flow at exit ($x=L$) for tracer in the various permeability fields

We will call this function "Koval" function and assume that it is a good representation for tracer displacement in a perfectly layered medium. This function defines the heterogeneity factor H which characterizes the importance of layered heterogeneities. Fractional flow is then given by the standard solution of Koval's equation (with continuous injection)

$$\begin{aligned} f(x,t) &= 0 & ; & \quad t < t_{\min} = x/Hu \\ f(x,t) &= 1 & ; & \quad t > t_{\max} = xH/u \\ f(x,t) &= \frac{H - \sqrt{Hx/ut}}{H-1} & ; & \quad t_{\min} < t < t_{\max} \end{aligned}$$

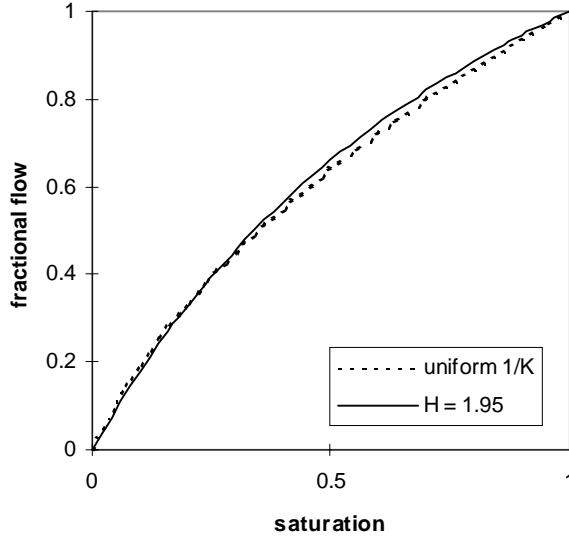


Fig. 12 - Fractional flow for a uniform distribution of $1/K$ (between 0.4 and 1.6) and approximation by a Koval function with $H=1.95$

The variance of the Koval fractional flow is easily derived

$$\sigma_f^2(x) = \frac{(H-1)^2}{3H} \frac{x^2}{u^2}$$

It must be noted that when we assume a certain form of the fractional flow, we actually assume a given permeability distribution $G(K)$ of the layers. For the Koval equation above,

$$G(K) = 0 \quad ; \quad K < K_{\min} = \langle K \rangle / H$$

$$G(K) = \frac{\sqrt{H}}{2(H-1)} \frac{K^{-1/2}}{\langle K \rangle^{-1/2}} \quad ; \quad K_{\min} < K < K_{\max}$$

$$G(K) = 0 \quad ; \quad K > K_{\max} = H \langle K \rangle$$

Using the two limiting expressions of standard dispersion and layering, a model based on the separation of scales, is used to derive the fractional flow for any intermediate correlation length.

4.2.2 Calculation of $f(x,t)$

In this section we determine a homogenized form of the fractional flow as a function of x and t . To do this, we define a two-scale model where the large scale heterogeneities are represented by layers with different permeabilities K_i , and the short-range correlations inside the layers are characterized by dispersivity D (Fig. 13). Using this model we can derive directly the terms A and B in the fractional flow variance, and the fractional flow as function of x and t .

The variance of fractional flow can be derived directly from the variance of arrival times

$$\sigma_f^2 = \frac{(H-1)^2}{3H} \frac{x^2}{u^2} + 2D \frac{x}{u^2} \frac{(H^2 + H + 1)}{3H}$$

leading to the values of A and B

$$A = \frac{1}{u^2} \frac{(H-1)^2}{3H} \quad ; \quad B = 2D \frac{1}{u^2} \frac{(H^2 + H + 1)}{3H}$$

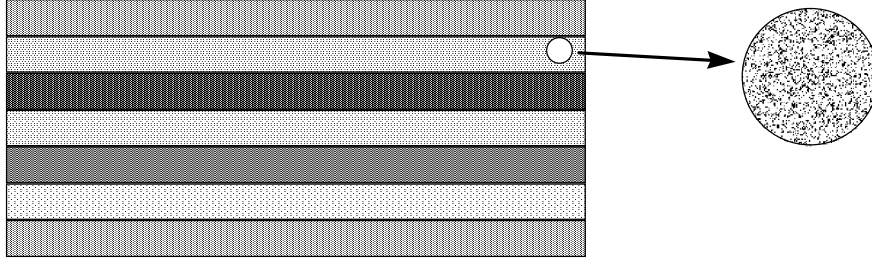


Fig. 13 - the two-scale models used to calculate fractional flow. The large scale heterogeneities are represented by layers with different permeabilities and short-range correlations by randomness inside the layers.

The fractional flow at distance x is calculated by summing the flux in each layer (error function) over all the layers. For each layer, the mean velocity u is function of permeability.

$$f(x, t) = \frac{1}{4} \int_{K_{\min}}^{K_{\max}} \left(\operatorname{erf} \left(\frac{u(K)t - x}{2x\sqrt{D/x}} \right) + 1 \right) \frac{\sqrt{H}}{H-1} \frac{K^{-1/2}}{\langle K \rangle^{-1/2}} dK$$

This integral equation is a homogenized form of the fractional flow. We can verify that the variance is the same as the one derived from the arrival times.

Fig. 14 shows the calculation of the two-scale model $f(x, t)$ at $x=L$ for different values of H and $D=0.05L$ as a function of pore volumes injected. Note that when $H=1$, the fractional flow follows the limiting case of pure dispersion, whereas when $H=4$, $f(x, t)$ is much closer to the Koval function. $H=2$ represents an intermediate case between the two extremes.

We can also compare our homogenized fractional flow model with results from numerical simulations. Fig. 15 shows comparisons between the two-scale model fractional flow (denoted MHD in the legend) and ATHOS. Fig. 15 compares simulations on two permeability fields of correlation length $\lambda=0.01$ and $\lambda=10$. The matches are quite satisfactory, and demonstrate that the two extreme cases are described well.

We have derived a homogenized form of the fractional flow of a tracer in the form $f(x, t)$ for a cross-sectional displacement. However this model does not provide a transport equation, which may be more useful for some upscaling applications.

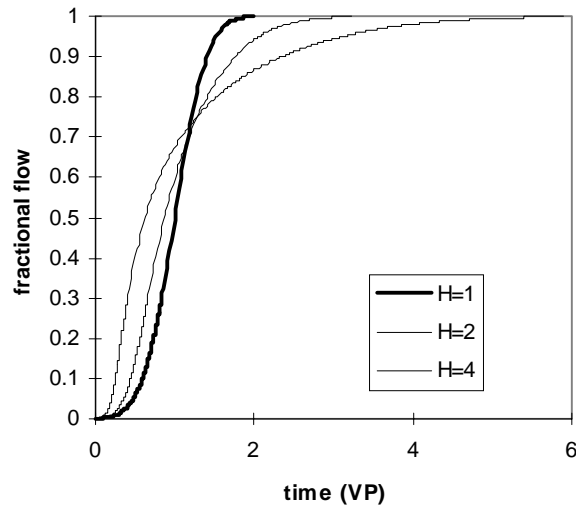


Fig. 14 - Fractional flow calculated with the convolution function for various heterogeneity factors and dispersivity $D=0.05 L$.

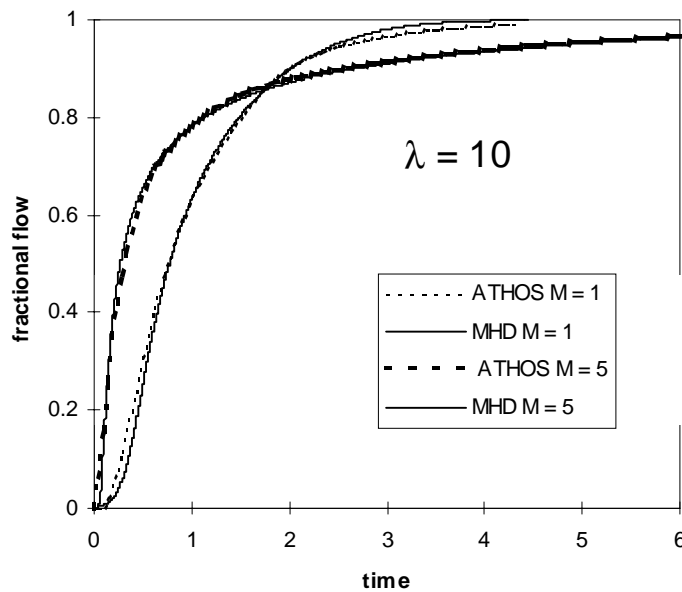


Fig. 15 - Comparison between flux calculated using the two-scale model and results of numerical simulations (with ATHOS), for correlation length $\lambda=0.01$ and $\lambda=10$.

4.2.3 Calculation of convective and dispersive fractional flows F_c and F_d

We have derive the fractional flow as function of distance and time. However, for scaling purposes, we may need a transport equation, derived from a relationship between flux and saturation. So far, we have not been able to derive the functions F_c and F_d using the two-scale model. We can propose empirical equations that agree with the limiting cases.

The first approach is to postulate that the two functions F_c and F_d are the same as for the limiting cases of purely dispersive and purely convective displacements.

$$F_c = \frac{S}{S + (1-S)/H} \quad ; \quad F_d = D$$

leading to the local transport equation

$$\frac{\partial S_i}{\partial t} + u \frac{\partial}{\partial x} \left(\frac{S}{S + (1-S)/H} \right) = uD \frac{\partial^2 S}{\partial x^2}$$

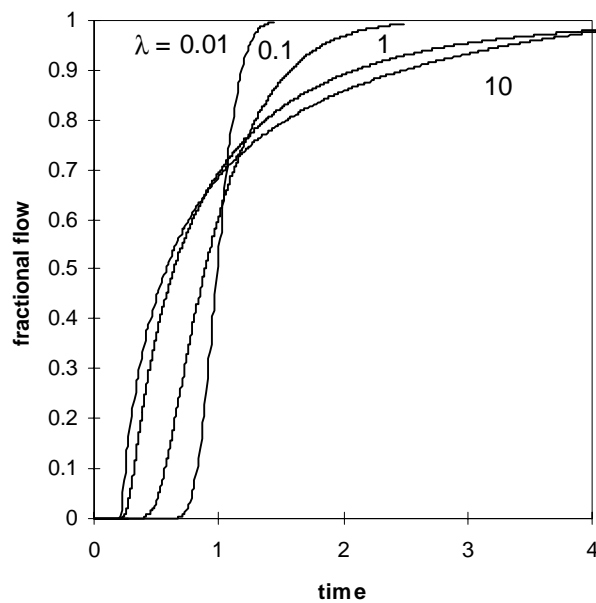


Fig. 16 - Simulation of fractional flow with the transport differential equation (first approach)

Fig. 16 shows the simulation results of this 1-dimensional transport equation for the fractional flow. The crossover between dispersive and convective regimes is in good agreement with numerical simulations and results of the two-scale model $f(x,t)$ in Fig. 14.

The second approach uses the transport equation in each streamtube in the two-scale model. For a streamtube number i , with dispersivity D and front velocity u_i , the saturation S_i follows the convection dispersion equation (CDE)

$$\frac{\partial S_i}{\partial t} + u_i \frac{\partial S_i}{\partial x} = u_i D \frac{\partial^2 S_i}{\partial x^2}$$

In order to add the contribution of all the streamtubes, the CDE equation must be written in terms of mass m of tracer, by multiplying each equation by the cross-section area a_i of the corresponding streamtube.

$$\frac{\partial m_i}{\partial t} + \frac{\partial a_i u_i S_i}{\partial x} = D \frac{\partial^2 a_i u_i S_i}{\partial x^2}$$

Assuming vertical equilibrium, the cross section a_i is inversely proportional to velocity u_i (in order to have the same pressure gradient along all the tubes). u is the average front velocity and a the total cross-section area

$$\frac{\partial m_i}{\partial t} + au \frac{\partial S_i}{\partial x} = Dau \frac{\partial^2 S_i}{\partial x^2}$$

The sum over all the tubes of the term m_i leads to the average saturation, but the sum of all the S_i cannot be related to flux or saturation. By analogy with the limiting case of purely layered medium, we postulate that this term is equal to

$$\sum_i u S_i = F_C = \frac{S}{S + (1-S)/H}$$

Consequently, the dispersive fractional flow is equal to

$$F_D = D \frac{dF_C}{dS}$$

This equation is more complicated than the first one, but it has the advantage to have analytical solutions (Yortsos and Fokas, 1980)

4.2.4 Remark

We have used the same notation H and D for three different approaches : the flux $f(x,t)$ derived from the two-scale model and for the two approaches for F_C and F_D calculation but the values of H and D are different. They will be determined to satisfy what we have called the "homogenization rules", i.e. the same scaling factors A and B .

4.2.5 Calculation of H and D

We have shown that using the parameters H and D we can predict the results from numerical simulations. We have not yet demonstrated how H and D are calculated. It is here that the rules for homogenization are applied, and the values of H and D are determined. The procedure is as follows:

- 1) Either from the theory (Section 4.1) or from fine grid simulations, the relationship $\sigma^2(x)$ is established
- 2) We then approximate $\sigma^2(x)$ by the polynomial $Ax^2 + Bx$, and the constants A and B are determined
- 3) Given the values A and B , we can then calculate the H and D such that the homogenized fractional flow is equivalent to $\sigma^2(x)$. When using the transport equations, H and B are determined by history matching. For the tracer case, this can be done using the result of the two scale model

$$A = \frac{1}{u^2} \frac{(H-1)^2}{3H} \quad ; \quad B = 2D \frac{1}{u^2} \frac{(H^2 + H + 1)}{3H}$$

5. Applications to Miscible Flow

We have shown that we were able to predict a transport equation and fractional flow for tracer injection. This is not only a first step before the study of more complicated flow (viscous effects, local Kr, Pc), but the tool to characterize the heterogeneity by two parameters H and D related to flow properties.

Our numerical simulations confirm the result established experimentally by Koval for miscible flows (1963) and more recently by Lenormand and Thiele (1996) for first-contact miscible fluids. The fractional flow derived for tracer can be used for displacements with viscosity contrasts by replacing H by the product HM^* where M^* is an effective mobility ratio. Fig. 17 demonstrates the effectiveness of this approach. In this figure, we compare simulation results using ATHOS with predictions of the fractional flow using the two scale model $f(x,t)$ and replacing H by the product HM^* .

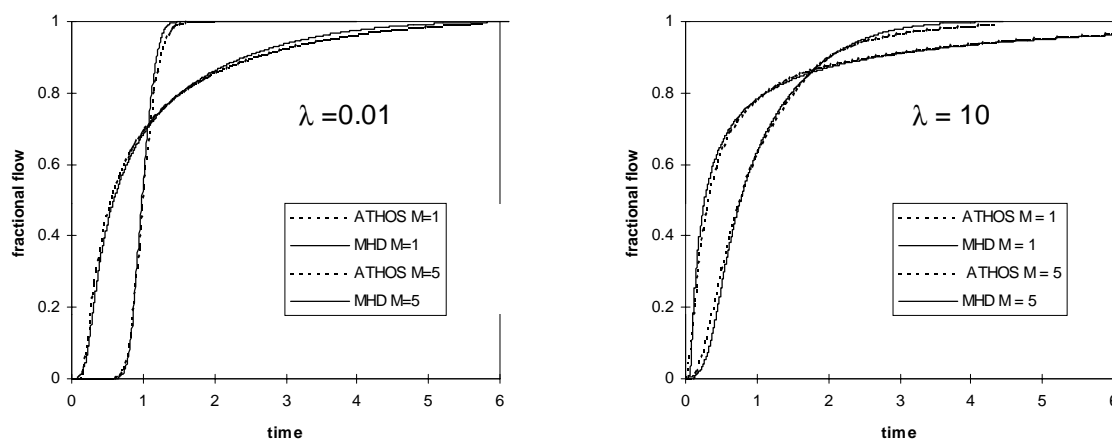


Fig. 17 - Effect of viscosity for $\lambda=0.01$ and $\lambda=10$: comparison between numerical simulations (ATHOS) the flux calculated with the two-scale model with $M^*= 2.2$.

For pressure equation, we can use an effective viscosity (or mobility) approach such as the one proposed by Todd and Longstaff (1972). The validity of this approach for first-contact miscible displacements has been demonstrated by Fayers et al. (1991).

6. Discussion and Conclusion

The main purpose of this study is two-phase upscaling in numerical simulator. The principle is to replace numerical upscaling (Kyte and Berry, 1975) by an analytical calculation of the average properties.

Our approach is based on homogenization of the saturation (or fractional flow) profiles instead of permeability. It will consist in the following steps:

- 1) **determination of the parameters A and B** that characterize the heterogeneous permeability field. The parameter A accounts for correlated heterogeneities in the mean flow direction and B for the uncorrelated randomness. These two parameters A and B

are derived either directly from the geostatistical properties of the field, if they are known (correlation length, fractal dimension, etc.) or determined from a numerical simulation of a tracer displacement if only one realization of the field is known. These two parameters are function of the size of the field.

- 2) **determination of the functions F_c , F_d and P** for a given process. These three functions are the convective and dispersive part of the fractional flow and the pressure equation. They will be determined (analytically or using tables), using the field properties A and B, and the fluids and flow conditions (local relative permeability and capillary pressure, viscosity ratio, flow rate, etc.). So far we have presented results for simple tracer flow. The fractional flow functions F_c and F_d are determined from A and B. In this case, the pressure gradient is the same as for a one-phase flow and is determined from the average permeability. Studies to include local relative permeabilities and capillary pressure are in progress.
- 3) **correction for discretization.** The principle is to treat numerical dispersion as physical dispersion. Preliminary results have shown that numerical dispersion could be corrected by reducing the value of B by a factor that can be calculated from grid size and time steps.
- 4) **calculation of pseudos $\langle K_r \rangle$ and $\langle P_c \rangle$.** From the three homogenized curves $F_c(S)$, $F_d(S)$ and $P(S)$, numerical calculation of the two pseudos relative permeabilities, and pseudo capillary pressure. We must emphasize that these pseudos used in the simulator are no longer properties similar to the local K_r or P_c . For instance, $\langle P_c \rangle$ will account for all the dispersive effects (for instance random heterogeneities), even if there is no local capillary pressure.

Acknowledgments

We would like to thank Y. Yortsos, M. Blunt and A. Bourgeat for helpful discussions and suggestions. We also thank the Petroleum Engineering Department at Stanford University for allowing us to use the 3DSL streamline simulator.

References

- Batycky, R.P., Blunt, M.J., and Thiele, M.R., A 3D Field-Scale Streamline-Based Reservoir Simulator, SPE Reservoir Engineering, **12**, 246-254, (1997)
- Chang, Y.C. and Mohanty, K.K., Stochastic Description of Multiphase Flow in Heterogeneous Media, SPE 28443, New Orleans, 1994
- Deutsch, C. V. and Journel, A. G., GSLIB Geostatistical Software Library And User's Guide, Oxford University Press (1992).
- Fayers, F. J., Blunt, M. J. and Christie, M. A., Accurate calibration of Empirical Viscous Fingering Models, Revue de l'Institut Français du Pétrole 46, 311-325, 1991
- Gelhar, L. W. and Axness, C. L., Three-Dimensional Stochastic Analysis Of Macrodispersion In Aquifers, Water Res. Res. **19**, 161-180, 1983.
- Glimm, J., Lindquist, F., Pereira, F. and Zhang, Q., A Theory Of Macrodispersion For The Scale Up Problem, Transp. Porous Media, **13**, 97-122, (1993).
- Koval, E. J., A method for Predicting the Performance of Unstable Miscible Displacements in Heterogeneous Media, Trans. AIME **228**, 145, 1963.
- Kyte, J. R. and Berry, D. W., New Pseudo Functions to Control Numerical Dispersion, Soc. Petr. Eng. J. **15**, 269-276, 1975.
- Lenormand, R., Use Of Fractional Derivatives For Fluid Flow In Heterogeneous Media, In: 3rd European Conference On The Mathematics Of Oil Recovery, Edited By Christie Et Al, Published By Delft University Press, Delft, The Netherlands, 1992.

- Lenormand, R., A Stream Tube Model For Miscible Flow, Part 1: Macrodispersion In Random Porous Media, *Transp. In Porous Media* **18**, 245-261, 1995.
- Lenormand, R., Determining Flow Equations from Stochastic Properties of a Permeability Field: the MHD Model, SPE 30797, *SPE J.* **1**, 1996.
- Lenormand, R. and Thiele, M., Homogenization Of Flow Equations Using The MHD Equation: Numerical Validation, Paper Presented At The 5th European Conference On The Mathematics Of Oil Recovery, Leoben, Austria, 1996.
- Lenormand, R. and Wang, B., A Stream Tube Model For Miscible Flow, Part 2: Macrodispersion In Porous Media With Long-Range Correlations, *Transp. In Porous Media* **18**, 263-282, 1995.
- Marle, C., Cours de production. Tome IV: les écoulements polyphasiques en milieux poreux, Technip, Paris 1972.
- Quintard, M. and Bertin, H., Two-Phase Flow In Heterogeneous Porous Media : The Method Of Large-Scale Averaging Applied To Laboratory Experiments In A Stratified System, SPE 1982, San Antonio, 1989.
- Todd, M. R. and Longstaff, W. J., The Development, Testing and Application of a numerical Simulator for Predicting Miscible Flood Performance, *Trans. AIME* **253**, 984, 1972.
- Yortsos, Y. and Fokas, S., An analytical solution for linear waterflood including the effects of capillary pressure, SPE 9407, Dallas, 1980.